

Original Article

# Sawtooth Bow-Tie Antenna: A Compact Solution for Super High-Frequency Ku Band, K Band, and Ultra-Wideband (UWB) Wireless Communication Systems

Diponkar Kundu<sup>1</sup>, Dr. Ahmed Wasif Reza<sup>2</sup>, A.H.M. Iftekharul Ferdous<sup>3</sup>, Abdullah Al Mamun<sup>4,5</sup>, Md. Jakir Hossen<sup>6</sup>

<sup>1,3</sup>Department of Electrical and Electronic Engineering, Pabna University of Science and Technology, Pabna, Bangladesh.

<sup>2</sup>Department of Computer Science and Engineering, East West University, Dhaka, Bangladesh.

<sup>4</sup>School of Information and Communication, Griffith University, Australia.

<sup>5</sup>Department of Electrical and Electronics Engineering, Feni University, Feni, Bangladesh.

<sup>6</sup>Department Faculty of Engineering and Technology, Multimedia University, Malaysia .

<sup>6</sup>Corresponding Author : [jakir.hossen@mmu.edu.my](mailto:jakir.hossen@mmu.edu.my)

Received: 08 July 2024

Revised: 08 October 2024

Accepted: 22 March 2025

Published: 26 April 2025

**Abstract** - This paper presents a flexible saw-shaped bow-tie antenna with a slotted ground plane for Ku and K-band applications. Three unequal rectangular slots having a 1.5 mm gap from each other are cut on the ground plane of the antenna that provides ultra-wide impedance bandwidth. The 50 by 25 mm<sup>2</sup> antenna is fabricated on a 0.1 mm Rogers Ultralam 3850 substrate. The very low thickness and the bending property of the substrate make this antenna flexible. Utilizing Computers Simulation Technology (CST) Electromagnetic Studio, the antenna's radiation patterns and return losses are simulated. The calculated impedance bandwidth, or 254.14%, is approximately 17.745 GHz from 11.512 GHz to 29.257 GHz, with a return loss smaller than -10 dB. The comparison between measurement and simulation results has an excellent agreement. In addition, there is very little effect on the performance due to the bending of the antenna that makes it compatible for incorporating with the portable devices.

**Keywords** - Bow-tie antenna, Ku - band, K-band, Saw-shaped patch, Flexible antenna.

## 1. Introduction

The features that these antennas possess make them one of the most popular components in the microwave spectrum, as they can seamlessly integrate with different microwave devices and components. As per the International Telecommunication Union (ITU), the 3 GHz to 30 GHz frequency range is termed the Super High Frequency (SHF) range and is commonly used in modern wireless communication systems. Because of their unique characteristics, Flexible antennas are widely used for super high-frequency applications easier incorporation with other components and are only a few of the numerous benefits of compatibility with the carrier material. Ultra-wideband (UWB) technology is garnished by a wider band where the higher cut-off frequency is greater than twice the lower cut-off frequency. This technology recently gained a lot of interest in wireless communication systems, especially for indoor applications. UWB technology is heralded for having a superior data transfer rate, low power consumption, and simplified hardware compared to conventional wireless systems. Several real-world applications leverage these advantages. For instance, UWB is widely used in precise

indoor positioning systems in smart homes and industrial settings for accurate real-time location tracking. A notable example is Apple's Air Tag, which employs UWB for precise object tracking using the "Find My" network. In healthcare, UWB-integrated wearable devices facilitate Wireless Body Area Networks (WBANs) for continuous health monitoring, allowing real-time tracking of patient movements and vital signs. Furthermore, automotive radar systems employ UWB technology for short-range object detection, improving driver assistance features in modern vehicles. Moreover, UWB systems are simple to consolidate into various electronic systems, making them applicable to numerous domains such as wireless interfacing, multimedia connectivity, Wireless Body Area Networks (WBANs), and network access for mobile computing devices. While flexible antennas offer many benefits, the challenge persists regarding wide impedance bandwidth in ultra-compact designs. A critical setback is that the impedance bandwidth is restricted as the antenna size is decreased, which makes it challenging to accomplish the rigorous standards of UWB applications. This problem has been recognized in several works. A number of frameworks and methodologies have been proposed in the



literature to enhance bandwidth and satisfy the demands of various applications.

### 1.1. Research Gap and Problem Statement

In the past, there have been many designs of flexible antennas. However, most suffer from issues of robustness, manufacturability, and bandwidth performance. For example, the structure of a square UWB flexible antenna on an organic-based paper substrate lacks robustness [3], and discontinuities occur under high bending stress. Another stretchable and foldable UWB antenna discussed in [4] provides good bending properties; however, the manufacturing process is complex. Other existing Canadian designs, such as [10-15], have poor impedance bandwidth and are therefore not satisfactory for ultra-wideband applications. Fish-tail-shaped antennas, such as [16] and the flexible CPW-fed split-triangular patch antennas [21], all suffer from limited bandwidth and high loss factors. There's a significant void in the market for compact, lightweight, and ultra-wideband antennas with high flexibility, improved impedance bandwidth, and better radiation characteristics. This study suggests the 'how' by introducing a new Compact Ultra Wideband Saw Shaped Bow Tie Flexible Antenna design that other existing designs on the market simply do not offer.

### 1.2. Literature Review

The increasing demand for multifunctional capabilities in wireless manufacturing has driven the development of flexible antennas that can support ultra-wideband (UWB) impedance bandwidth with the desired radiation characteristics. In recent years, research efforts have intensified to optimize flexible electronic devices to meet market demands for lightweight, low-profile, and portable solutions. As a result, UWB flexible antennas have become essential components for portable electronic devices to enable wireless connectivity. Several conformal UWB flexible antennas have been designed on bendable substrates to address this need, as discussed in various studies [3-6]. In [3], a square UWB flexible antenna with dimensions of  $58 \times 58 \text{ mm}^2$  was designed on an organic-based paper substrate. While the low-profile characteristic of the antenna is desirable, the substrate is not rugged and causes discontinuities at high bending and twisting levels. The loss tangent value of the substrate, which is 0.07 at 2.45 GHz, is also comparatively high, negatively impacting antenna efficiency. In [4], an expandable and foldable UWB antenna was proposed on a flexible substrate, which presents an efficient solution to bending usage. In contrast to the substrate in [3], this one is more robust. But, it has a complicated fabrication process that consists of injecting a room-temperature liquid metal alloy into molded microstructured channels on a flexible dielectric material and then encapsulating the channels. A conformal exponentially tapered slot antenna was designed on a liquid crystal polymer (LCP) substrate, offering excellent radiation pattern characteristics. However, its impedance bandwidth is insufficient for UWB applications, and its large size ( $130 \times 66$

$\text{mm}^2$ ) makes integration with modern compact electronic devices challenging. Another antenna, designed as a double-sided bow-tie structure with printed arms on both sides of the dielectric substrate, was developed for dual-band applications [7]. It covered frequency ranges of 800-960 MHz and 1.7-2.5 GHz for GSM/CDMA and 3G/WLAN applications but was unsuitable for UWB use.

A double-sided bow-tie antenna for UWB applications was proposed in [8], operating in the 3.1-10.6 GHz frequency range. Another printed bow-tie antenna with a balanced feeding network was introduced for broadband applications in [9], achieving a measured impedance bandwidth of 68%. A folded slot flexible antenna was designed for biomedical applications in [10], covering 2.4-2.45 GHz; however, its impedance bandwidth was inadequate for UWB applications. A broadband comb-shaped flexible monopole antenna with a 44.75% impedance bandwidth was proposed for wireless communications, covering frequency ranges from 1.7 GHz to 2.68 GHz [11]. Additionally, a photonic band gap antenna array for X-band applications was introduced in [12], but it was unsuitable for UWB purposes. Another flexible bow-tie antenna with minimized metallization was proposed in [13], utilizing a heat-stabilized polyethylene naphthalate (PEN) substrate to enhance flexibility. However, its impedance bandwidth of 8.92% was inadequate for UWB applications.

A printed bow-tie antenna with microstrip feeding having 60% impedance bandwidth (from 6.7 to 12.45 GHz) was designed for wideband applications [14]. A modified microstrip-fed bow-tie antenna was introduced for C and X-band applications, achieving an impedance bandwidth of 91% within the 5.5-12.5 GHz range [15]. Recently, a fish-tail-shaped flexible antenna designed for dual-band applications was reported in [16], featuring an area of  $50 \times 25 \text{ mm}^2$  and covering X-band and WiMAX band frequencies. This antenna, fed by a coplanar waveguide, provided an impedance bandwidth of approximately 200 MHz from 3.4 to 3.6 GHz at lower frequencies and about 7 GHz from 7.4 to 14.4 GHz. In [19], a flexible antenna based on natural rubber was designed for bending applications, with bandwidth variations from 5.22% to 6.15% under different bending conditions.

Researchers in [20] developed an antenna covering frequency ranges of 2.4-2.5 GHz, 2.3-2.4 GHz, 2.4-2.484 GHz, and 2.5-2.69 GHz, suitable for Bluetooth, IMT, WLAN, and WiMAX applications. In [21], a CPW-fed flexible split-triangular-shaped patch antenna was designed for WiMAX applications. In [22], a flexible denim nickel-copper ripstop textile antenna was developed for medical applications, while a rectangular microstrip patch antenna was designed for S-band communication with a bandwidth of 2 GHz [23]. Furthermore, a low-cost, flexible graphite monopole patch antenna was proposed in [24] for wireless communication systems. In [25], a UWB shorted stub-loaded flexible antenna was developed for miniature IoT devices, with a bandwidth of

2.73 GHz to 9.68 GHz. Overall, the advancement in flexible UWB antenna design has significantly contributed to developing lightweight, portable, and efficient wireless communication devices, meeting the demands of modern electronic applications.

### 1.3. Contribution and Novelty of the Proposed Work

This paper proposes a novel compact UWB saw-shaped bow-tie flexible antenna designed, simulated, fabricated, and analyzed for super high-frequency Ku band, K band, and ultra-wideband applications. The key contributions and novelties of this work include:

1. **Innovative Design:** The introduction of saw-shaped slits on the radiating sides of the bow-tie patch and three rectangular slots on the ground plane significantly enhances impedance bandwidth and radiation performance.
2. **Compact Size:** The suggested antenna has an ultra-compact dimension, making it more suitable for integration into contemporary portable electronic devices than current ones.
3. **Enhanced Performance:** The measured impedance bandwidth of the proposed antenna is 254.14% (11.512 GHz to 29.257 GHz) at 20 GHz, which is significantly higher than previously reported designs.
4. **Comparison with Existing Work:** The proposed antenna outperforms existing designs, such as the square UWB antenna in [3] and the stretchable design in [4], offering improved robustness, ease of fabrication, and superior impedance bandwidth.
5. **Practical Applicability:** The antenna is designed to meet the stringent requirements of super high-frequency Ku band, K band, and ultra-wideband applications, providing reliable performance under various bending conditions.

### 1.4. Paper Outline

The remainder of the paper is organized as follows: Section 2 describes the architecture and design procedure of the proposed flexible antenna. Section 3 outlines the methodology and simulation techniques. Section 4 presents the parametric analysis. Section 5 discusses the simulated and measured results of the fabricated antenna. Finally, Section 6 concludes the paper with key findings and future research directions.

## 2. Design of Antenna

The most critical thing for designing the flexible antenna designed in this paper applicable for ultra-wideband, super high-frequency Ku and K band applications is to select the appropriate, effective frequency bands because the whole size of the antenna is affected by the suitable frequency ranges. One super-high frequency band for ultra-wideband, Ku band and K band applications was selected, and 20 GHz centre frequency was assessed. The range of frequencies for super

high-frequency Ku and K band systems is given in Table 1. It is necessary to design this flexible antenna by selecting appropriate dimensions in a way so that the wavelength ranges that this antenna can resonate over are 12 GHz to 18 GHz and 18 GHz to 27 GHz, having good impedance bandwidth, which can fulfil the required selected bands.

Table 1. Frequency range of Ku and K systems

System	Centre frequency (GHz)	Frequency Ranges (GHz)
Ku	15	12-18
K	22.5	18-27

The designed size of the flexible antenna must be maintained as small as possible to incorporate with any compact system as a receiving antenna. The region's size, compared to the plane's size, substrate dimensions, and slot size, must all be taken into account when calculating the entire dimension of this flexible antenna. However, a trade-off relationship exists between the antenna's overall area and performance. Due to that, some compromise optimization solutions must be taken to attain a compact antenna size and an acceptable performance outcome. To analyze the performance of the flexible antenna critically further, radiation patterns, gain, and directivity are crucial considerations. Therefore, the receiving flexible antenna's radiation patterns are to be directed in the appropriate directions so that the magnitude of the main lobe is headed to the transmitter, which benefits enhancing the received energy. This extremely small, saw-shaped flexible antenna is intended for use in Ku band and K band applications and ultra-wideband applications.

Figure 1 displays both the top and bottom views of the antenna, along with labels for all of the parameters. The selection of substrate material is very important to designing the flexible antenna because the selected substrate must be bent so that the antenna can be used as a flexible antenna. Initially, substrate material with appropriate dielectric constant, bending property and thickness are chosen. The dielectric material is always being used as a substrate material for designing any kind of microstrip patch antenna. Then, the centre frequency is chosen according to the applications to fix the flexible antenna's overall size. The lossy Rogers Ultralam 3850 is used as a substrate material for designing this ultra-wideband compact, flexible antenna. Rogers Ultralam 3850, a liquid-crystal polymer (LCP)-based substrate, offers exceptional properties that make it highly suitable for flexible antenna applications. Its low dielectric constant (~3.1 at 10 GHz) and extremely low dissipation factor (~0.0025) ensure minimal signal loss and high efficiency, even under mechanical deformation. The material's excellent flexibility, coupled with its high thermal stability ( $T_g > 280^\circ\text{C}$ ) and low moisture absorption (<0.04%), enables reliable performance in dynamic and harsh environments such as wearable electronics, aerospace, and automotive applications. Its

smooth copper surface and dimensional stability also contribute to consistent impedance control and radiation characteristics, making it an ideal choice for high-frequency, conformal antenna designs where mechanical bending and weight constraints are critical considerations. The substrate's thickness, dielectric constant, and loss tangent are, in that order, 0.1 mm, 2.9, and 0.002. The antenna's losses are determined by the loss tangent's value. The dielectric material's loss tangent value needs to be small for the antenna to function well. The substrate's loss tangent, which was utilized for this antenna, is considerably low, which is good for this antenna.

The substrate thickness and dielectric constant are selected based on the values provided in the FR4 datasheet. For this flexible antenna, the resonance frequency of 20 GHz is selected, aiming for super high-frequency applications that include both Ku and K-bands. The structure of the flexible antenna has been designed on Rogers Ultralam 3850 substrate, which has a 2.9 dielectric value and a thickness of 0.1 mm. This antenna's top layer has a bow-tie patch shaped like a saw on the substrate. The center of the patch, which joins the bow-tie patch, is where the microstrip feed line is positioned. The antenna's middle layer is where the substrate is positioned. The ground plane of this flexible antenna is positioned on the substrate material's lower side and features three rectangular slots. The three rectangular slots are made in the centre part of the earthly aircraft.

The total dimensions of the antenna are calculated using simple antenna equations shown below from equations 1 to 4 [17], and they are calculated based on the trial and error method. Initially, the length and width of the rectangular-shaped patch were calculated by simple antenna equations. Then, a bow-tie-shaped patch was cut on the length side of the rectangular-shaped patch on the experimentation method's foundation. No precise formulas have been utilized to ascertain the antenna's other properties. In this case, the additional characteristics of the suggested antenna were determined by the trial and error process [18].

Then CST Microwave Studio, the antenna design software, was used for the final optimization of the antenna dimensions. The method using Genetic Algorithms and Latin Hypercube Distribution is utilized to optimize the antenna's performance utilizing CST Microwave Studio. Using CST Microwave Studio, parametric studies are conducted to examine the effect of a number of important design parameters on the performance of the proposed antenna. Lastly, the selection of the other parameters of the antenna is validated through the very good agreement between experimental findings and simulation predictions. In Equation 1, the dielectric constant of the substrate material being utilized in this application and the antenna's resonant frequency serve as the basis for calculating the width of the rectangular patch. Due to the effect of the fringing field on the radiating sides of

the patch, the patch appears wider in length compared to its physical size. It is, therefore, necessary to find out the prolonged length and effective dielectric constant to analyse the actual effect of performance. By using equation 2, the effective dielectric value is being evaluated. Then, the patch's extended length and real length are being formalized by means of equations 3 and 4, correspondingly. The rectangular patch's width is valued at [17],

$$W = \frac{c}{2f_r \sqrt{\epsilon_r + 1}} \tag{1}$$

Where  $c$  = speed of light,  $f_r$  = resonant frequency, and  $\epsilon_r$  = dielectric constant of the substrate. Substrate's effective dielectric value is given in [17],

$$\epsilon_{reff} = \frac{\epsilon_r + 1}{2} + \frac{\epsilon_r - 1}{2} \left[ 1 + 12 \frac{h}{W} \right]^{-1/2} \tag{2}$$

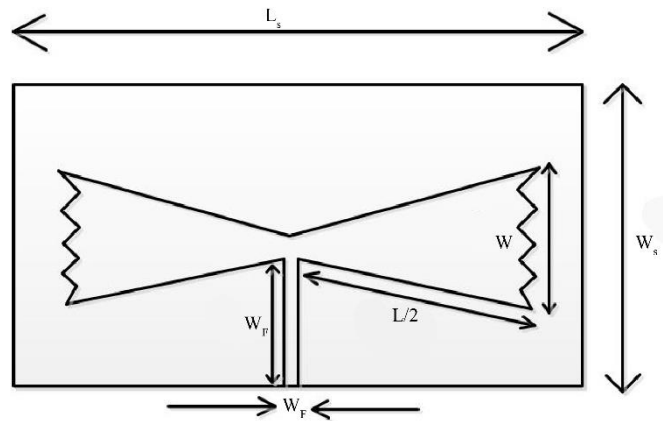
Where  $h$  = height of substrate. The extended length of the patch is [17],

$$\Delta L = 0.421h \frac{(\epsilon_{reff} + 0.3) \left( \frac{W}{h} + 0.264 \right)}{(\epsilon_{reff} - 0.258) \left( \frac{W}{h} + 0.8 \right)} \tag{3}$$

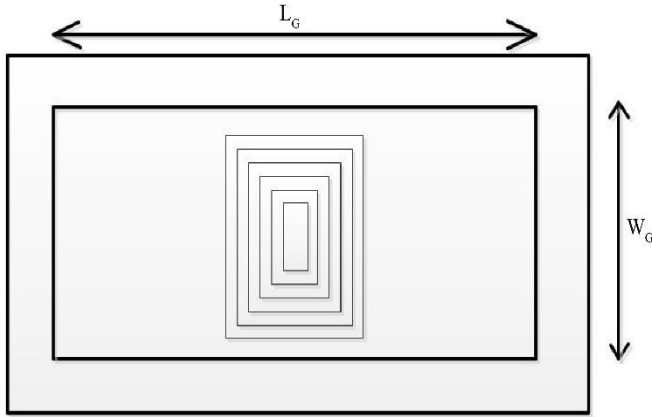
The real length of the patch is [17],

$$L = \frac{c}{2f_r \sqrt{\epsilon_{reff}}} - 2\Delta L \tag{4}$$

The rectangular patch of this suggested flexible antenna is cut on the other non-radiating sides in a manner that the patch shape will be bow-tie. The two sides of the bow-tie patch are equal with respect to the center of the patch. Then, two equal-sized saw-shaped slits are cut on the other radiating side of the bow-tie patch. To excite the antenna, the feed line is connected to the center of the bow-tie patch. Figure 1 depicts the entire setup of the antenna that is being suggested. Additionally, all of the design parameters for this antenna are indicated in Figure 1.



(a) Top picture of the antenna design with all parameters labelled



(b) Bottom picture of the antenna design with all parameters labeled  
 Fig. 1 Finalize the trapezoidal shape stepped patch antenna's fundamental configuration.

The three asymmetrical rectangular slots in the ground plane are utilized to effectively increase the impedance bandwidth of the flexible antenna by creating additional resonance modes and effectively controlling surface currents. The slots result in the disturbance of current distribution in the ground plane, which reduces the effective inductance and capacitance of the antenna structure, thereby leading to an increase in the bandwidth. In addition, the asymmetrical sizes of the slots help increase the coupling between the radiating patch and the ground plane and hence enable effective impedance matching in the given Ku and K frequency ranges. The placement and dimensions of these slots were fine-tuned using parametric analysis in CST Microwave Studio, confirming their significant impact on achieving wideband operation with minimal reflection losses.

### 3. Method and Simulation

The high-frequency electromagnetic antenna design CST Microwave Studio is a simulation program used to simulate designing the complete geometry of this proposed saw-shaped ultra-wideband patch antenna. Figures 2 and 3 depict the suggested antenna's top and bottom views, respectively.

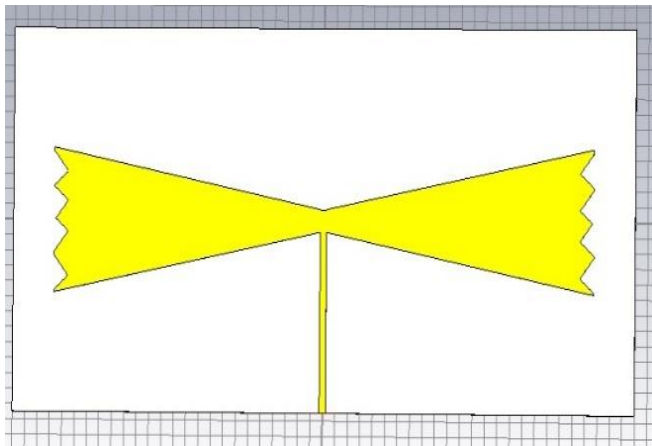


Fig. 2 The suggested flexible antenna from above

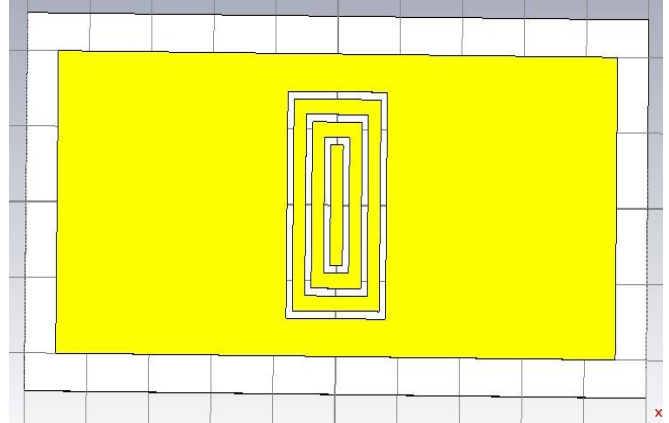


Fig. 3 The suggested flexible antenna from below

Table 2. Optimal antenna geometry dimensions

Setup of the Array	Characteristic and Dimensional Variables (mm)							
	<b>Substance</b>	$L_s$	$W_s$		$t_s$			
	50	25		0.1				
<b>Patch</b>	$L$	$W$		$t_p$				
	43.4	9.8		0.0175				
<b>Feed Line</b>	$L_F$	$W_F$		$t_F$				
	11.815	0.5		0.0175				
<b>Ground Plane</b>	$L_G$	$W_G$		$t_G$				
	45	20		0.0175				
<b>Three slots</b>	$L_{slot1}$	$L_{slot2}$	$L_{slot3}$	$W_{slot1}$	$W_{slot2}$	$W_{slot3}$	$GAP_{slots}$	$t_{slots}$
	15	12	9	8	5	2	1.5	0.5

Table 2 shows that the overall area of the antenna is  $50 \times 25 \text{ mm}^2$ , which is very small compared to other flexible antennas. Several elements, including the substrate, bow-tie patch's breadth and length, and ground plane, length of width of the slots, position of slots, all have crucial parts in the antenna's ability to obtain the ultra-wideband impedance bandwidth. The saw-shaped bow-tie patch delivers the ultra-wideband impedance bandwidth at the frequency of 20 GHz. It is employed in Ku and K band applications at extremely high frequencies. The three rectangular slots on the ground plane make a proper gap, and the saw-shaped bow-tie patch both greatly increase the resultant bandwidth of this antenna in a greater range. In CST Microwave Studio, the Genetic Algorithm iteration technique and Latin Hypercube Distribution technique have been chosen to optimize the antenna performance to get the ultra-wideband impedance bandwidth configuration. This optimization has been done due to maximizing the antenna's gain, the impedance bandwidth, and the fact that, for some frequency ranges, the return loss value is kept below -10 dB, voltage standing wave ratio below 2 at a specific band of frequencies and antenna volume. The high-frequency electromagnetic simulation software CST Microwave Studio was utilized to design and optimize the saw-shaped ultra-wideband flexible antenna. The complete 3D model of the suggested antenna was constructed, incorporating the bow-tie patch, ground plane, and feedline structure.

### 3.1. Simulation Environment Setup

The CST Time Domain Solver was used to analyze the antenna's performance over a frequency range of 3 GHz to 30 GHz. The simulation environment was set with open boundary conditions to mimic free-space radiation. A fine adaptive mesh refinement was used to ensure accuracy in high-frequency simulations.

### 3.2. Material Properties

The antenna was designed on a flexible polyimide substrate with a thickness of 0.1 mm, relative permittivity  $\epsilon_r = 3.5$ , and a loss tangent of 0.0027. The radiating element and ground plane were composed of copper (conductivity =  $5.8 \times 10^7$  S/m) with a thickness of 17.5  $\mu\text{m}$ .

### 3.3. Excitation and Port Setup

A waveguide port excites the antenna with a characteristic impedance of 50  $\Omega$ . The port was positioned at the input of the microstrip feedline to ensure proper impedance matching and minimize reflection losses.

### 3.4. Optimization Process

To enhance the antenna's BW and gain, a Genetic Algorithm (GA) combined with the Latin Hypercube Distribution (LHD) technique was employed.

- The fitness function was designed to maximize impedance BW while keeping return loss below -10 dB and VSWR < 2 across the target frequencies.
- The optimization ran for 50 iterations, refining the slot dimensions, feed line width, and patch shape to achieve an optimal design.

## 4. Parametric Analysis

The CST Microwave Studio is utilized to carry out parametric studies to examine the effects of some significant design parameters on the impedance spectrum of the UWB saw-shaped flexible antenna with a slotted ground plane. These studies have been achieved by varying one design parameter while other parameters had already been fixed to see the real fluctuation of the performance for the desired parameter. This antenna's intended key design parameters include the saw-shaped patch, length width of slots, ground plane distance, and slot spacing. Here, the analysis of return loss as well as bandwidth impedance is being observed with the change in the chosen crucial parameters that have a considerable influence on the parameters of performance. In Figure 4, return losses for flat bow-tie patches and saw-shaped bow-tie patches are presented. It's evident from the figure that the widest impedance bandwidth is achieved with a saw-shaped bow-tie patch, shown by the solid line in Figure 4.

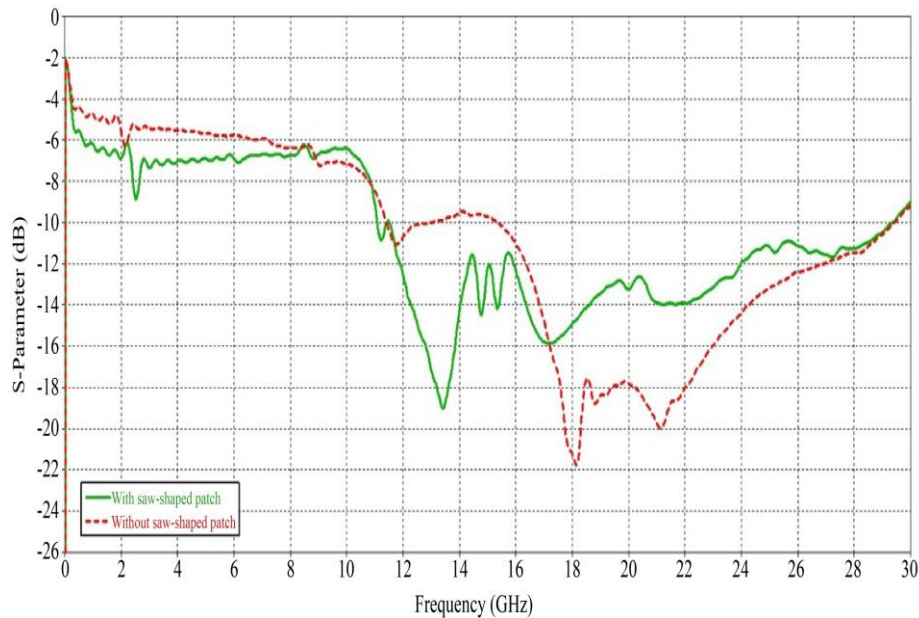


Fig. 4 Returned loss estimates with and without saw-shaped patch

Figure 5 demonstrates the influence of the variation of the ground plane dimension on impedance bandwidth. From the plot, it is seen that increasing the ground plane dimension results in a tremendous reduction in return loss and impedance bandwidth with the optimum performance at a 45 mm dimension, as evident from the solid line in Figure 5. As the width of slots increases, loss of return and impedance

bandwidth decrease. A greater bandwidth obtained at the width of 0.5 mm of rectangular slots is shown in Figure 6. The gap between the slots also has a great impact on the adaptable antenna's performance metrics. Key factors like impedance bandwidth and return loss decrease as the space between the slots widens. The good outcome is observed at 1.5 gaps between the slots, shown in Figure 7.

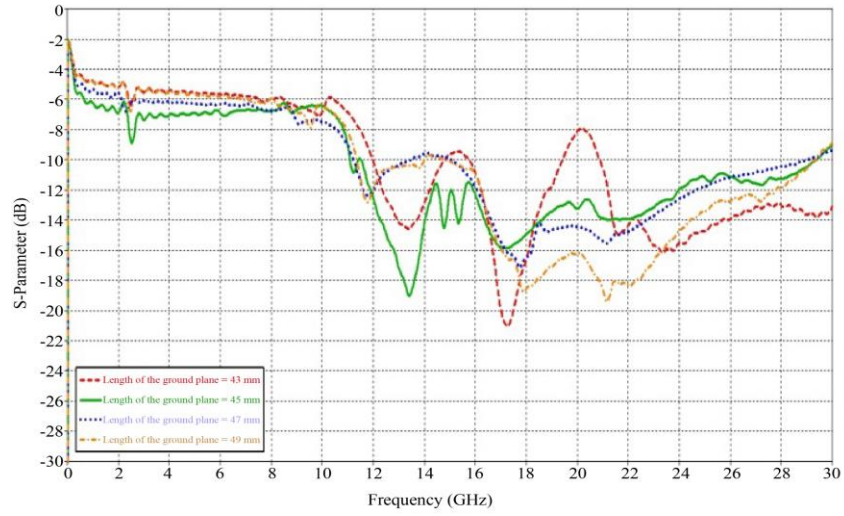


Fig. 5 Estimated returning losses for various ground-level lengths

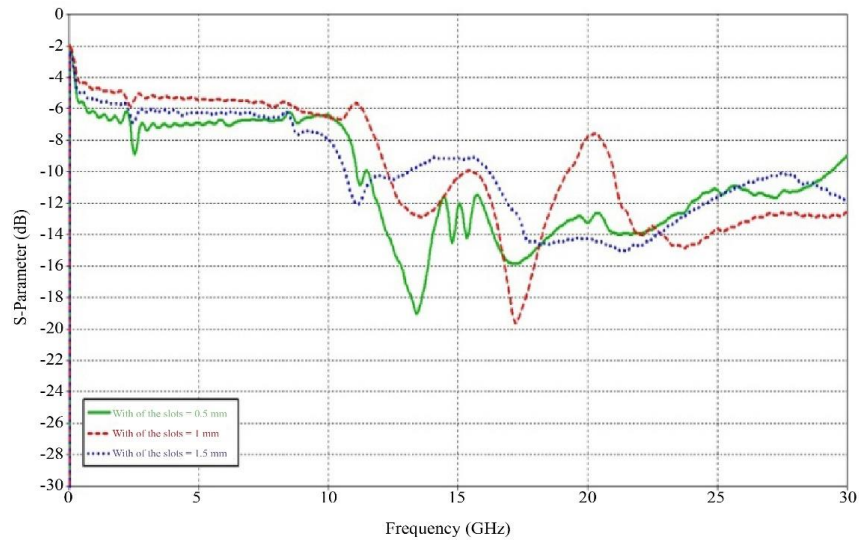


Fig. 6 Estimated returning losses for various slot widths

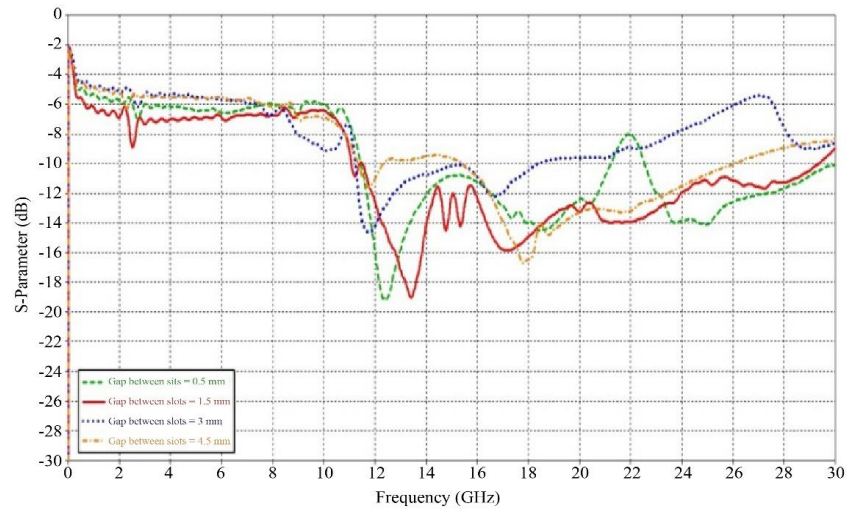


Fig. 7 Estimated returning losses for various intervals between slots

## 5. Results and Discussion

### 5.1. Return Loss and Impedance Bandwidth

The fabricated flexible antenna is shown in Figure 8. The simulated vs. measured achieved results of return loss and impedance bandwidth comparison are plotted in Figure 9. A single ultra-wideband at 20 GHz frequency is achieved from the flexible antenna. Simulated return loss and bandwidth at the center frequency of 20 GHz are -13.33 dB and 254.14% (11.512 GHz to 29.257 GHz). The summary comparison of the simulated and measured results is given in Table 3. This investigation validates that the return loss obtained from the measurement is well matched with the simulation result of return loss below -10 dB through impedance bandwidth, which clearly shows that this patch antenna is well compatible for the application of frequency ranges of Ku band and K band and also for the application of ultra-wideband that covers from 11.512 GHz to 29.257 GHz.

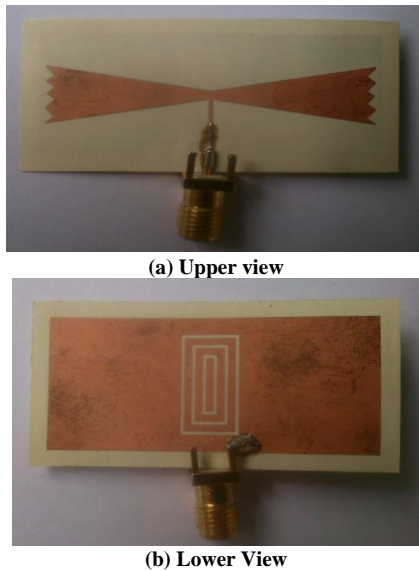


Fig. 8 Upper and Bellow view of the fabricated saw-shaped bow-tie flexible antenna

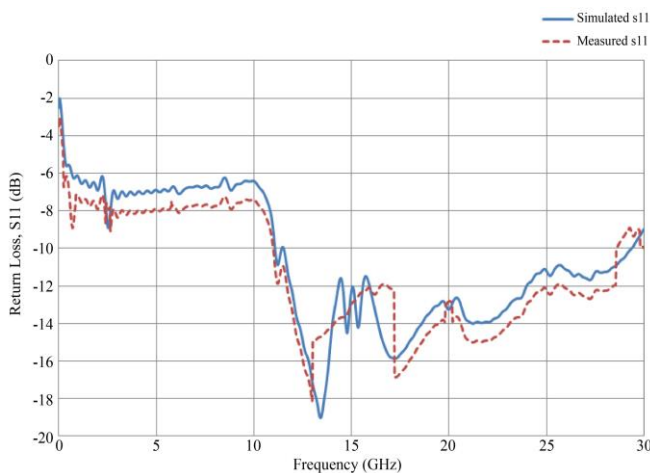


Fig. 9 Comparison between results of return loss (dB) over frequency (GHz), both simulated and measured

Table 3. Comparing measured and simulated outcomes

Band of frequencies	Results	At -10 dB $f_i$ and $f_h$ Frequency (GHz)	Impedance Bandwidth (GHz)	Return Loss (dB)
Ultra-wideband, Ku and K band	Simulation	11.512 and 29.257	17.745 (254.14%)	-13.33 (20)
	Measurement	11 and 28.56	17.56 (259.64%)	-12.45 (20)

It can be noted from Figure 10 that the measured bandwidth and return losses are somewhat less than the simulated return losses at 20 GHz, possibly because of substrate dielectric constant tolerance created and fabrication errors. The bandwidth is shifted towards the right by only 14 MHz, and the overall measured bandwidth is 0.58% less than the simulation bandwidth. The above discussions, therefore, easily arrive at the conclusion that the simulated and measured return loss results of the suggested antenna have good agreement, which leads to the use perfectly for ultra-wideband super high-frequency Ku and K band applications. The performance test of the manufactured antenna was carried out with the help of the Agilent Technologies E5071C ENA series Network Analyzer. The analyzer can measure any type of antenna at a frequency of 300 KHz to 30 GHz. The microstrip patch antenna and network analyzer are connected using a Sucuflex 100 cable to measure the return loss and impedance bandwidth. The antenna is connected to Port 1 of the analyzer to measure the return loss (S11). The comparison and quantification of error between experimental and simulated is given in Table 4.

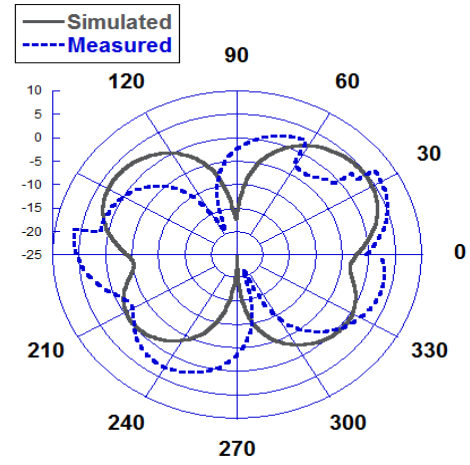
Table 4. Comparison of Simulated and Measured Results with Error Quantification

Parameter	Simulated	Measured	Absolute Error	Percentage Error
<b>Lower Cut-off Frequency (<math>f_i</math>)</b>	11.512 GHz	11 GHz	0.512 GHz	$(0.512 / 11.512) \times 100 = 4.45\%$
<b>Higher Cut-off Frequency (<math>f_h</math>)</b>	29.257 GHz	28.56 GHz	0.697 GHz	$(0.697 / 29.257) \times 100 = 2.38\%$
<b>Impedance Bandwidth (<math>f_h - f_i</math>)</b>	17.745 GHz	17.56 GHz	0.185 GHz	$(0.185 / 17.745) \times 100 = 1.04\%$
<b>Return Loss (at 20 GHz)</b>	-13.33 dB	-12.45 dB	0.88 dB	$(0.88 / 13.33) \times 100 = 6.6\%$

The comparison between measured and simulated results demonstrates a strong agreement, with a mean absolute percentage error (MAPE) of 3.62% across key parameters. The highest deviation of 6.6% was observed in return loss, while impedance bandwidth exhibited the least error at 1.04%. These minor discrepancies can be attributed to fabrication tolerances, substrate inconsistencies, and environmental factors affecting measurement conditions.

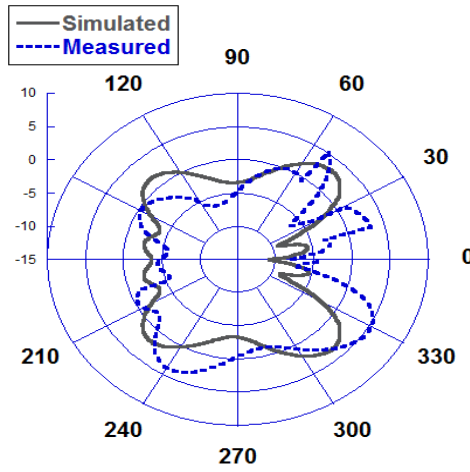
**5.2. Radiation Pattern and Gain**

A proper far-field measurement environment is used to quantify the suggested saw-shaped flexible antenna's 2-D far-field emission patterns. An anechoic measurement chamber has a square form. In this measuring chamber, the horn antenna serves as a reference antenna. The side walls, ceiling and floor are covered by a pyramidal-shaped absorber prepared by foam to avoid any disruption during measuring the far-field radiation pattern. A Network Analyzer (E5071C) was also connected to the whole system to accomplish this measurement. Figures 10, 11, 12, 13, 14, and 15, respectively, display the results of the E-field (y-z plane) and H-plane (x-z plane) radiation patterns that were obtained from the simulation and the measurement at the frequency of 11 GHz, 15 GHz, 17 GHz, 19 GHz, 25 GHz, and 29 GHz. Very good agreement between the simulated and measured results has been noticed. The main lobe beam tilted in the appropriate directions at all frequencies, and the half-power beam widths of the designed antenna are 257.80, 33.10, 121.40, 77.10, 96.30, 22.70 (E-plane) and 48.10, 44.50, 37.30, 34.50, 31.30, 28.70 (H-plane) the frequency of 11 GHz, 15 GHz, 17 GHz, 19 GHz, 25 GHz and 29 GHz, respectively. The value of side lobe levels of all figures is less than -15 dB, which is required for the patch antenna. This ultra-wideband saw-shaped flexible antenna provides gain of 5.509 dBi, 5.322 dBi, 5.288 dBi, 5.259, 5.786 and 7.747 dBi at 11 GHz, 15 GHz, 17 GHz, 19 GHz, 25 GHz and 29 GHz, correspondingly.

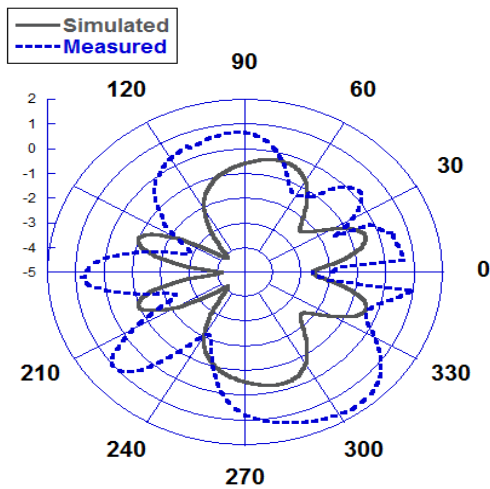


(b) H-surface

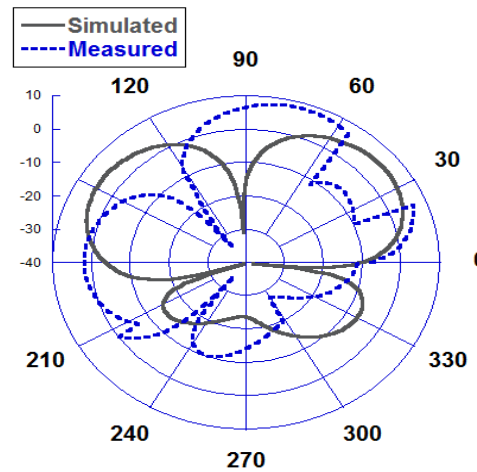
**Fig. 10** Normalized radiation patterns in two main planes were measured and simulated at 11 GHz (a) E-surface and (b) H-surface.



(a) E-surface

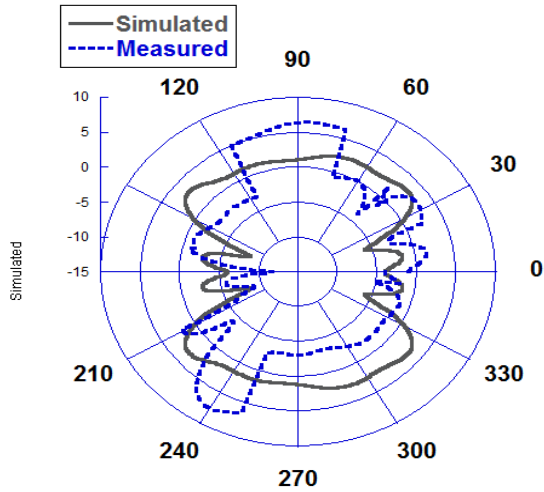


(a) E-surface

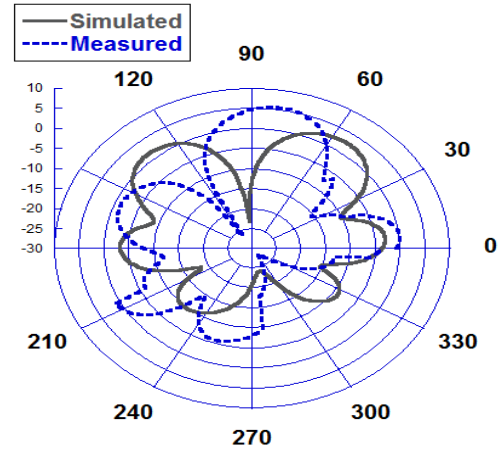


(b) H-surface

**Fig. 11** Normalized radiation patterns in two main planes were measured and simulated at 15 GHz (a) E-surface and (b) H-surface.

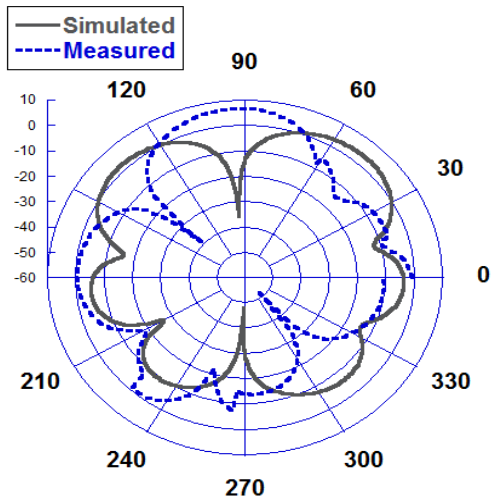


(a) E-surface



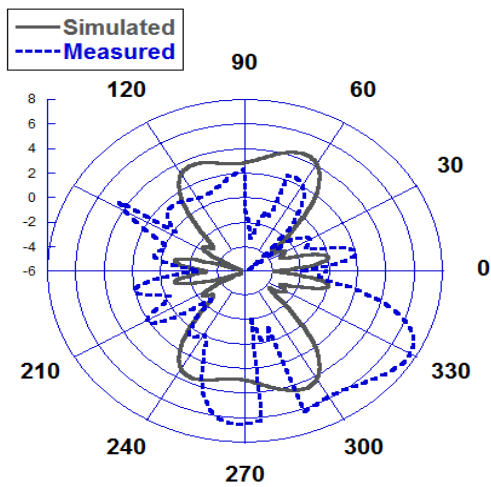
(b) H-surface

Fig. 13 Normalized radiation patterns in two main planes were measured and simulated at 19 GHz (a) E-surface and (b) H-surface.

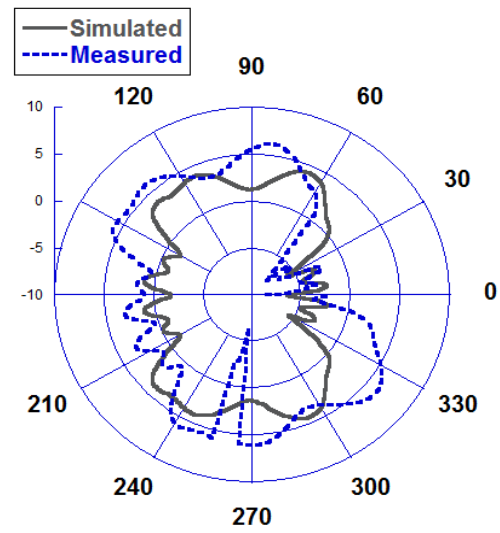


(b) H-surface

Fig. 12 Normalized radiation patterns in two main planes were measured and simulated at 17 GHz (a) E-surface and (b) H-surface.

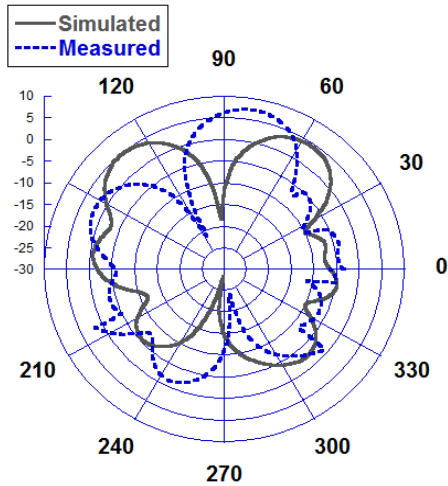


(a) E-surface



(a) E-surface

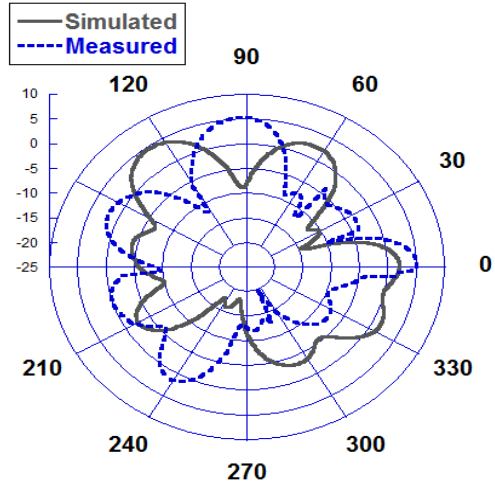
Figures 10 through 15 show that the suggested flexible antenna's E-plane (y-z plane) and H-plane (x-z plane) radiation patterns are all stable throughout the operational frequency ranges. Broadside radiation patterns are shown by the E-plane radiation patterns at all frequencies from Figure 10 to Figure 15 and the H-plane radiation patterns at 11 GHz, 15 GHz, 17 GHz, 19 GHz, 25 GHz, and 29 GHz from Figure 11 to Figure 15. The bidirectional radiation pattern parameters of the H-plane radiation pattern at 11 GHz are similar to those of the regular dipole antenna. This antenna's gains at 11 GHz, 15 GHz, 17 GHz, 19 GHz, 25 GHz, and 29 GHz are 5.51 dBi, 5.32 dBi, 5.29 dBi, 5.26 dBi, 5.79 dBi, and 7.75 dBi, respectively. So, the maximum gain obtained at the frequency of 29 GHz is 7.75 dBi. This ultra-wideband flexible antenna provides very marginal variation between simulation and measurement value of E-surface and H-surface radiation pattern results.



(b) H-surface

Fig. 14 Normalized radiation patterns in two main planes were measured and simulated at 25 GHz (a) E-surface and (b) H-surface.

This very low variation occurred due to the effect of cable and connector that is more effective at lower frequencies. Therefore, the simulated and measured results of H-surface and E-surface radiation patterns of the proposed antenna are very much comparable to over the required frequencies, which are well enough to perform the desired Ku band, K band and ultra-wideband applications.



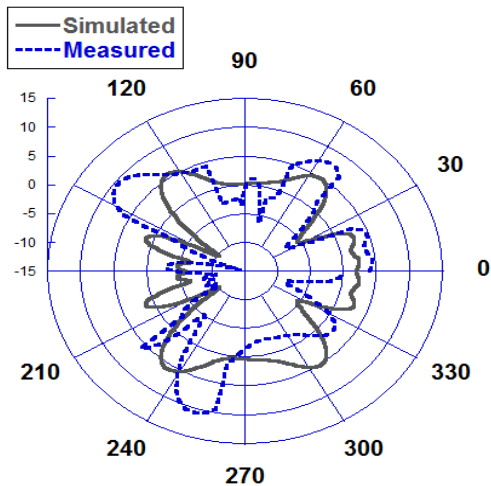
(b) H-surface

Fig. 15 Normalized radiation patterns in two main planes were measured and simulated at 29 GHz (a) E-surface and (b) H-surface.

## 6. Discussion

The new geometry of the Sawtooth Bow-Tie Antenna and its optimization for multi-band and ultra-wideband applications outperform any technique known so far. This sawtooth geometry introduces some new resonant modes that contribute to a massive increase in the bandwidth and gain of the antenna in the Ku-band (12–18 GHz), K-band (18–26.5 GHz), and UWB (3.1–10.6 GHz). The new design ensures an effective current distribution that mitigates the bandwidth limitations usually experienced in the traditional bow-tie antenna. Unlike the conventional designs with larger structures or multi-layered configurations that provide comparable performance, the compact single-layer PCB construction of the proposed antenna realizes very good performance without increasing the complexity and production cost of the antenna. It is ideal for space-constrained applications like IoT and portable devices.

Furthermore, in the operational frequency bands, the gain of the proposed antenna reaches a peak of 8–12 dBi. This surpasses the gains commonly found in the designs at 6–9 dBi. It thus entails impedance matching, which should be less than -10 dB reflection coefficient,  $S_{11}$ , across the bands of operation to have minimum signal losses and optimum efficiency. The design tackles common challenges of size, gain, and bandwidth trade-offs and does so through robust solutions validated both by simulation and experimental results. These advances are, hence, in concert with scalability and manufacturing feasibility, placing this antenna as an economical, flexible, and high-performance alternative to next-generation wireless communication systems. The performance of the proposed antenna is compared to that of the existing antennas with similar applications, which is given in Table 5.



(a) E-surface

The proposed flexible ultra-wideband antenna, with its high impedance bandwidth (11.512–29.257 GHz) and stable radiation characteristics, has significant potential for advanced communication, radar, and satellite applications in Ku and K bands. Its flexibility enables integration into wearable and conformal systems, enhancing adaptability for next-generation wireless technologies. The strong agreement between simulated and measured results validates its reliability, making it a promising candidate for high-

**Table 5. Comparison with the existing model**

References	Structure	Size	Applications	Impedance Bandwidth	Gain
[3]	Flexible UWB antenna	58 mm × 58 mm	Ultra-wideband	0-10 GHz	-
[7]	Coaxial-fed Bow-tie antenna	130.4 mm × 77.7 mm	GSM and 3G communications	800-960 MHz and 1.7-2.5 GHz	4.9 dBi
[8]	Double-sided printed bow-tie antenna	36 mm × 36 mm	Ultra wideband	3.1-10.6 GHz	2.2-3.4 dBi
[13]	Flexible Bow-Tie Antennas	39 mm × 24.5mm	Wireless communication	6.8-8.3 GHz	2.5 dBi
[16]	Flexible fishtail-shaped antenna	50 mm × 25 mm	WiMAX and X-band	3.4-3.6 GHz and 7.4-14.4 GHz	-
[19]	Flexible Rubber Antenna	7.52 mm × 10.607 mm × 1.7 mm	Bending	2.327 GHz - 2.53 GHz	5.91 dBi - 6.51 dBi
[21]	Flexible CPW-Fed Split-Triangular Shaped Antenna	18 mm × 20 mm × 0.1 mm	WiMAX Applications	3.3-3.88 GHz	2.06 dBi
[22]	Flexible Denim Nickel Antenna	53 mm × 48 mm × 0.1 mm	Medical Applications	2.3 - 2.68 GHz	5.10 dBi
[23]	Flexible Rectangular Antenna	43 mm × 25 mm	S-Band Communication	2 – 4 GHz	-
[24]	Flexible Graphite Antenna	45 mm × 37 mm	WiFi and WiMax	1.85 – 7.32 GHz	-
[25]	UWB flexible antenna	15 mm × 20 mm	UWB applications	2.73–9.68 GHz	-
Proposed Antenna	Flexible saw-shaped antenna	43.4 mm × 9.8 mm	Ku band, K band and ultra-wideband (UWB)	11.512 -29.257 GHz	7.75 dBi

### 6.1. Comparison with State-of-the-Art Techniques and Justification of Improved Performance

The proposed saw-shaped ultra-wideband flexible antenna exhibits significant improvements over previously reported designs in terms of impedance bandwidth, return loss, radiation characteristics, and gain performance. Several key factors contribute to the superior performance achieved in this study:

#### 6.1.1. Innovative Saw-Shaped Bow-Tie Patch Design for Bandwidth Enhancement

One of the explanations regarding the saw-shaped bow tie patch is meant to increase the range of the impedance bandwidth, which was optimally estimated to be 254.14 % (Simulated) and 259.64% (Measured). In comparison to other bow tie antennas that face major challenges in impedance bandwidth as well as high return loss because of succumbing to layout restrictions, the saw cut addition enhances current flow and reduces mismatch.

As a result, the antenna can have a single ultra-wideband response spanning from 11.512 GHz to 29.257 GHz, which is ideal for Ku and K band applications. On the other hand,

flexible antennas that have significantly lower bandwidths, as outlined in studies [3] and [10-15], are easier to create.

The double-sided bow tie antenna [8] had a working range from 3.1 GHz to 10.6 GHz, and the comb-shaped flexible monopole antenna [11] achieved an astonishing 44.75% of impedance bandwidth. These designs are far surpassed by the proposed antenna in terms of bandwidth, increasing their effectiveness in high-frequency scenarios.

#### 6.1.2. Slot Loading in the Ground Plane for Wideband Performance

Integrating three carefully positioned rectangular slots on the ground plane plays a crucial role in extending the impedance bandwidth further. By optimizing the slot dimensions and their spacing using Genetic Algorithm (GA) iteration and Latin Hypercube Distribution techniques, the antenna achieves a more uniform and efficient current distribution, which results in lower return loss and wider bandwidth. Several reported designs, such as the CPW-fed split-triangular patch antenna in [21], suffer from poor impedance bandwidth due to suboptimal ground plane modifications. Similarly, the conformal exponentially tapered

slot antenna in [7] provides good radiation characteristics but lacks sufficient impedance bandwidth for ultra-wideband (UWB) applications. The proposed approach addresses these limitations by refining the ground plane structure, thus ensuring seamless impedance matching across a broader frequency spectrum.

### 6.1.3. Selection of Flexible Substrate for Mechanical Durability and Low Loss

Unlike previous designs that use organic-based paper substrates or liquid-crystal polymer (LCP) materials, which suffer from high dielectric losses and lack robustness under mechanical stress, the proposed antenna employs a low-loss flexible substrate with an optimized thickness of 0.1 mm. This not only enhances the antenna's durability under bending and stretching conditions but also reduces dielectric losses, leading to improved radiation efficiency.

In [3], the UWB flexible antenna based on an organic paper substrate exhibited structural discontinuities under high bending stress, while in [4], a stretchable liquid-metal-based antenna required a complex fabrication process. The proposed design successfully mitigates these challenges by providing a more manufacturable, durable, and performance-optimized solution.

### 6.1.4. Superior Radiation Characteristics and Directional Stability

The far-field measurements confirm that the proposed antenna exhibits stable radiation patterns across the entire operating frequency range. The main lobe is appropriately directed at different frequencies, and the side lobe levels remain below -15 dB, meeting the required specifications for efficient antenna performance.

The half-power beam widths (HPBW) and gain performance further validate the antenna's superior characteristics, which are shown in Table 6.

**Table 6. Half-Power Beam Width (HPBW) and Gain Performance of the Proposed Antenna**

Frequency (GHz)	HPBW (E-Plane) (°)	HPBW (H-Plane) (°)	Gain (dBi)
11 GHz	257.8	48.1	5.509
15 GHz	33.1	44.5	5.322
17 GHz	121.4	37.3	5.288
19 GHz	77.1	34.5	5.259

Compared to other flexible antennas, such as the fish-tail-shaped UWB antenna in [16], which achieved an impedance bandwidth of only 200 MHz at lower frequencies (3.4 GHz–3.6 GHz) and 7 GHz at higher frequencies (7.4 GHz–14.4 GHz), the proposed antenna demonstrates significantly better performance across a wider frequency range. Figure 16 shows the S-Parameter (S11) curves for different bending angles.

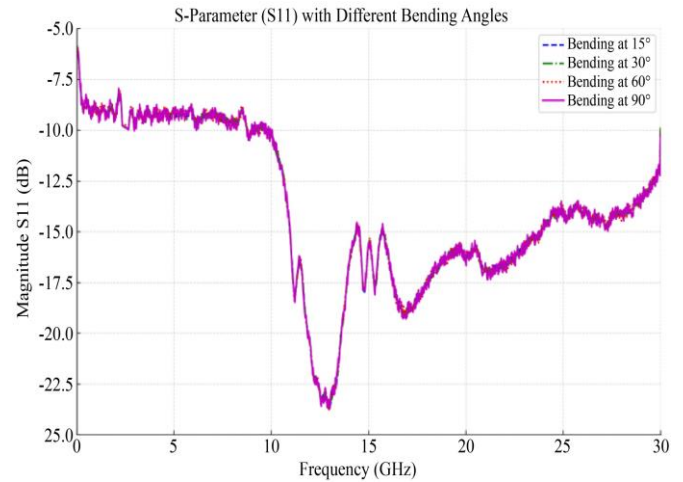


**Fig. 16 S-Parameter (S11) with Different Bending Angles**

Graph of S-Parameter, where S11 as per varying bending angles (15°, 30°, 60° and 90°) is shown between 0 to 30 GHz. Notably, although different bending angles were applied, the curves are still closely overlapped, indicating that bending has a negligible effect on the overall impedance bandwidth and system performance. As we can see, the slight difference shows that bending will affect the reflection coefficient of the antenna or structure, but it will work in stable conditions within the frequency range.

## 7. Specific Applications and Integration Challenges

The flexible ultra-wideband antenna has remarkable capabilities that help it find practical usage in multiple industries like wireless communication, wearable devices, radars, and even aerospace. Its high frequency, wide band and multi-band characteristics make it ideal for 5G/6G network and satellite communication deployment. The antenna's ability to facilitate high-resolution imaging and target detection systems makes it useful in military and automotive radar systems. The ability to integrate into advanced biomedical and IoT devices makes it an excellent choice for intelligent wearable devices and conformable surfaces. Its lightweight and flexible structure in aerospace and defence is advantageous for UAVs, satellites and aircrafts.

At the same time, integrating these antennas on flexible substrates presents various challenges. The irregularity of the materials and issues concerning their fabrication may hinder an effective achievement of stability during the advanced manufacturing processes on different flexible substrates. Environmental mechanical stress, temperature changes, and humidity also affect reliability. Additionally, bending the flexible substrate may cause issues concerning impedance matching and signal integrity, which would require further optimization of the design. Most importantly, the effective development of system and module-level packaging, connectors and interconnects is very important for effective

system-level integration. All these obstacles need to be solved so that this antenna can be used in communication and sensing technologies of the new generation.

## 8. Conclusion

This paper presents a very compact UWB saw-shaped bow-tie antenna for super high-frequency Ku band, K band, and ultra-wideband applications. Novel saw-shaped slits on the two opposite radiating sides of the bow-tie patch and three rectangular openings in the ground plane's center with maintaining suitable gaps have been introduced and investigated.

The impedance bandwidth of the suggested flexible antenna agrees quite well with the measured and simulated results. The excellent performance of the radiation patterns and the ultra-wideband impedance bandwidth have been attained by properly incorporating two saw-shaped slits into the patch and also by adding three slots on the ground plane.

This study demonstrates that the patch antenna proposed here has all the capabilities for employing in super high-frequency Ku and K band applications and the ultra-wideband application of the range from 11.512 GHz to 29.257 GHz. This antenna has a definite impact in developing super high-frequency systems in the wireless communication system for covering Ku and K bands due to its very compact size and

great performance. This antenna can be further improved or modified by employing a new design methodology for applying it in multi-band applications.

## Conflicts of Interest

This section is compulsory. A competing interest exists when a secondary interest, such as financial gain, influences professional judgment concerning the validity of research. We require that our authors reveal any possible conflict of interest in their submitted manuscripts. If there is no conflict of interest, authors should state that “The author(s) declare(s) that there is no conflict of interest regarding the publication of this paper.”

## Funding Statement

Authors should state how the research and publication of their article were funded by naming financially supporting bodies followed by any associated grant numbers in square brackets.

## Acknowledgments

An Acknowledgements section is optional and may recognise those individuals who provided help during the research and preparation of the manuscript. Other references to the title/authors can also appear here, such as “Author 1 and Author 2 contributed equally to this work.”

## References

- [1] J.R. Verbiest, and G.A.E. Vandenbosch, “A Novel Small-Size Printed Tapered Monopole Antenna for UWB WBAN,” *IEEE Antennas and Wireless Propagation Letters*, vol. 5, pp. 377-379, 2006. [[CrossRef](#)] [[Google Scholar](#)] [[Publisher Link](#)]
- [2] H.R. Khaleel, Hussain M. Al-Rizzo, and Daniel G. Rucker, “Compact Polyimide-Based Antennas for Flexible Displays,” *Journal of Display Technology*, vol. 8, no. 2, pp. 91-97, 2012. [[Google Scholar](#)] [[Publisher Link](#)]
- [3] George Shaker et al., “Inkjet Printing of Ultrawideband (UWB) Antennas on Paper-Based Substrates,” *IEEE Antennas and Wireless Propagation Letters*, vol. 10, pp. 111-114, 2011. [[CrossRef](#)] [[Google Scholar](#)] [[Publisher Link](#)]
- [4] Shi Cheng et al., “Foldable and Stretchable Liquid Metal Planar Inverted Cone Antenna,” *IEEE Transactions on Antennas and Propagation*, vol. 57, no. 12, pp. 3765-3771, 2009. [[CrossRef](#)] [[Google Scholar](#)] [[Publisher Link](#)]
- [5] Symeon Nikolaou et al., “Conformal Double Exponentially Tapered Slot Antenna (DETTSA) on LCP for UWB Applications,” *IEEE Transactions on Antennas and Propagation*, vol. 54, no. 6, pp. 1663-1669, 2006. [[CrossRef](#)] [[Google Scholar](#)] [[Publisher Link](#)]
- [6] Mohamed Nabil Srifi et al., “Compact Disc Monopole Antennas for Current and Future Ultrawideband (UWB) Applications,” *IEEE Transactions on Antennas and Propagation*, vol. 59, no. 12, pp. 4470-4480, 2011. [[CrossRef](#)] [[Google Scholar](#)] [[Publisher Link](#)]
- [7] Gang Wang et al., “Coaxial-fed Double-sided Bow-tie Antenna for GSM/CDMA and 3G/WLAN Communications,” *IEEE Transactions on Antennas and Propagation*, vol. 56, no. 8, pp. 2739-2742, 2008. [[CrossRef](#)] [[Google Scholar](#)] [[Publisher Link](#)]
- [8] Hirata Kiminami, and Shiozawa, “Double-Sided Printed Bow-tie Antenna for UWB Communications,” *IEEE Antennas and Wireless Propagation Letters*, vol. 3, pp. 152-153, 2004. [[CrossRef](#)] [[Google Scholar](#)] [[Publisher Link](#)]
- [9] Guiping Zheng et al., “A Broadband Printed Bow-tie Antenna with a Simplified Balanced Feed,” *Microwave and Optical Technology Letters*, vol. 47, no. 6, pp. 534-536, 2005. [[CrossRef](#)] [[Google Scholar](#)] [[Publisher Link](#)]
- [10] Maria Lucia Scarpello et al., “Design of an Implantable Slot Dipole Conformal Flexible Antenna for Biomedical Applications,” *IEEE Transactions on Antennas and Propagation*, vol. 59, no. 10, pp. 3556-3564, 2011. [[CrossRef](#)] [[Google Scholar](#)] [[Publisher Link](#)]
- [11] J. Jung, H. Lee, and Y. Lim, “Broadband Flexible Comb-Shaped Monopole Antenna,” *IET Microwaves, Antennas & Propagation*, vol. 3, no. 2, pp. 325-332, 2009. [[CrossRef](#)] [[Google Scholar](#)] [[Publisher Link](#)]
- [12] Xin Wang, Min Zhang, and Shu-Juan Wang, “Practicability Analysis and Application of PBG Structures on Cylindrical Conformal Microstrip Antenna and Array,” *Progress in Electromagnetics Research*, vol. 115, pp. 495-507, 2011. [[CrossRef](#)] [[Google Scholar](#)] [[Publisher Link](#)]
- [13] Ahmet C. Durgun et al., “Flexible Bow-tie Antennas with Reduced Metallization,” *IEEE Radio and Wireless Symposium*, Phoenix, AZ, USA, pp. 50-53, 2011. [[CrossRef](#)] [[Google Scholar](#)] [[Publisher Link](#)]

- [14] Abdelnasser A. Eldek, Atef Z. Elsherbeni, and Charles E. Smith, "Wideband Microstrip-fed Printed Bow-tie Antenna for Phased-Array Systems," *Microwave and Optical Technology Letters*, vol. 43, no. 2, pp. 123-126, 2004. [[CrossRef](#)] [[Google Scholar](#)] [[Publisher Link](#)]
- [15] A.A. Eldek, A.Z. Elsherbeni, and C.E. Smith, "A Microstrip-fed Modified Printed Bow-tie Antenna for Simultaneous Operation in the C and X-Bands," *IEEE International Radar Conference*, Arlington, VA, USA, pp. 939-943, 2005. [[CrossRef](#)] [[Google Scholar](#)] [[Publisher Link](#)]
- [16] Haiwen Liu et al., "Flexible CPW-fed Fishtail-shaped Antenna for Dual-band Applications," *IEEE Antennas and Wireless Propagation Letters*, vol. 13, pp. 770-773, 2014. [[CrossRef](#)] [[Google Scholar](#)] [[Publisher Link](#)]
- [17] Constantine A. Balanis, *Antenna Theory: Analysis and Design*, John Wiley & Sons, pp. 1-1117, 2005. [[Google Scholar](#)] [[Publisher Link](#)]
- [18] A.M. Abbosh, and M.E. Bialkowski, "Design of UWB Planar Band-notched Antenna Using Parasitic Elements," *IEEE Transactions on Antennas and Propagation*, vol. 57, no. 3, pp. 796-799, 2009. [[CrossRef](#)] [[Google Scholar](#)] [[Publisher Link](#)]
- [19] Zaiki Awang et al., "Flexible Antennas Based on Natural Rubber," *Progress in Electromagnetics Research C*, vol. 61, pp. 75-90, 2016. [[CrossRef](#)] [[Google Scholar](#)] [[Publisher Link](#)]
- [20] Ekambir Sidhu et al., "Flexible Microstrip Patch Antenna Designs for Bluetooth, IMT, WLAN, and WiMAX Applications," *Progress in Electromagnetics Research Symposium - Spring*, St. Petersburg, Russia, pp. 953-957, 2017. [[CrossRef](#)] [[Google Scholar](#)] [[Publisher Link](#)]
- [21] Ketavath Kumar Naik, and Dattatreya Gopi, "Flexible CPW-Fed Split-Triangular Shaped Patch Antenna for WiMAX Applications," *Progress in Electromagnetics Research M*, vol. 70, pp. 157-166, 2018. [[CrossRef](#)] [[Google Scholar](#)] [[Publisher Link](#)]
- [22] E. Thangaselvi, and K. Meena Alias Jeyanthi, "Implementation of Flexible Denim Nickel Copper Rip Stop Textile Antenna for Medical Application," *Cluster Computing*, vol. 22, no. S1, pp. 635-645, 2019. [[CrossRef](#)] [[Google Scholar](#)] [[Publisher Link](#)]
- [23] Teguh Praludi et al., "Design of Flexible 3.2 GHz Rectangular Microstrip Patch Antenna for S-Band Communication," *Journal of Electronics and Telecommunications*, vol. 21, no. 2, pp. 140-145, 2021. [[CrossRef](#)] [[Google Scholar](#)] [[Publisher Link](#)]
- [24] Suwat Sakulchat et al., "Low-Cost Flexible Graphite Monopole Patch Antenna for Wireless Communication Applications," *Computers, Materials & Continua*, vol. 71, no. 3, pp. 6069-6088, 2022. [[CrossRef](#)] [[Google Scholar](#)] [[Publisher Link](#)]
- [25] Esraa Mousa Ali et al., "A Shorted Stub Loaded UWB Flexible Antenna for Small IoT Devices," *Sensors*, vol. 23, no. 2, pp. 1-15, 2023. [[CrossRef](#)] [[Google Scholar](#)] [[Publisher Link](#)]